

Avoided Quantum Tricritical Point and Emergence of a Canted Magnetic Phase in $\text{LaCr}_{1-x}\text{Fe}_x\text{Sb}_3$

R. R. Ullah,¹ J. S. Harvey,¹ H. Jin,¹ Y. Wu,² H. B. Cao,² J. R. Badger,³ P. Klavins,¹ and V. Taufour¹

¹Department of Physics and Astronomy, University of California Davis, Davis, California 95616, USA

²Neutron Scattering Division, Oak Ridge National Laboratory, Oak Ridge, Tennessee 37831, USA

³Department of Chemistry, University of California Davis, Davis, California 95616, USA

(Received 18 December 2023; revised 22 July 2024; accepted 30 July 2024; published 27 August 2024)

New phases or new phenomena are often observed near-zero temperature phase transitions. These new effects represent nature's way of avoiding quantum critical phase transitions. Here, we look at the quantum tricritical point (QTCP), the special case where two transitions are driven to zero temperature at the same time. Unlike the case of quantum critical points, the avoidance of quantum tricritical points has yet to be demonstrated. Using chemical substitution and a magnetic field, we drive LaCrSb_3 toward a quantum tricritical point. For the first time near a QTCP, we observe the emergence of a new magnetic phase and the avoidance of the QTCP via a first order phase transition.

DOI: 10.1103/PhysRevLett.133.096701

With pressure, strain, chemical substitution, or magnetic fields, one can sometimes drive a magnetic phase transition toward a quantum critical point (QCP), i.e., a second order transition at 0 K. Before such a QCP can be reached, however, new phases often appear. The antiferromagnetic (AFM) QCP, for example, is avoided by the appearance of a superconducting dome in the cuprate, Fe-based, and heavy fermion superconductors [1–4], resulting in the phase diagram sketched in Fig. 1(a).

The ferromagnetic (FM) QCP can also be avoided by a superconducting dome [5,6], but other phenomena are also possible. For example, there can be a tricritical point where the FM transition changes from second to first order. In such a case, quantum criticality is not completely suppressed and can reappear under a magnetic field. When a magnetic field is applied along the easy axis of magnetization, tricritical wings emerge, as illustrated in Fig. 1(b) [7–10]. The wings are bounded by second order lines that can terminate at 0 K at quantum wing critical points (QWCPs). In contrast to a QCP, no symmetry is broken at a QWCP. If the wing is accompanied by a Lifshitz transition, it will terminate at a marginal quantum critical point (MQCP) [11]. The FM-QCP can also be avoided by the appearance of an antiferromagnetic phase (AFM_Q) [7,12–23]. The avoidance of the FM-QCP by tricritical wings or by the appearance of an AFM_Q phase is theoretically expected to be a generic result for metallic quantum ferromagnets [7,24–29], with the exception of systems that are noncentrosymmetric [30–32] or one-dimensional [33,34] or that have disorder [35,36].

The avoidance of an FM-QCP by an AFM_Q phase can lead to yet another type of quantum criticality: if the wing terminates within the AFM_Q dome, there could be a quantum tricritical point (QTCP) as depicted in

Fig. 1(c) [17,37–42], where the zero-temperature transition from AFM_Q to a field-polarized state changes from the first to the second order. At a QTCP, both FM and AFM_Q fluctuations are expected to diverge simultaneously. In contrast to FM or AFM_Q -QCPs, few studies are aimed at approaching QTCPs. A QTCP was proposed in the phase

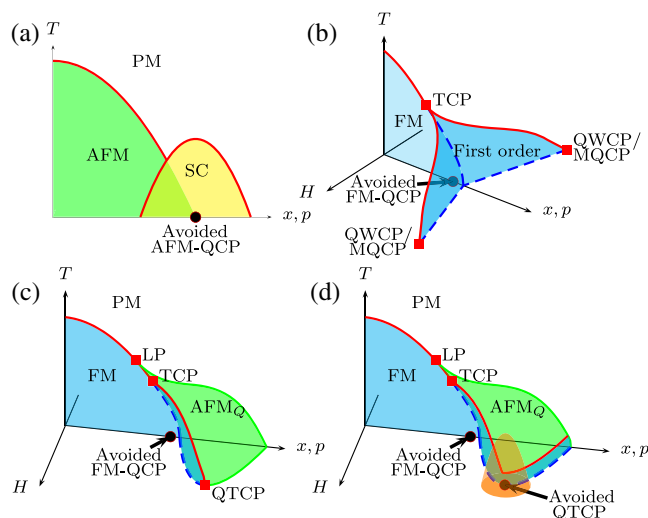


FIG. 1. Schematic phase diagrams of avoided quantum critical points (QCP). (a) Antiferromagnetic (AFM) case with the emergence of superconductivity (SC). (b)–(d) Ferromagnetic (FM) cases with the emergence of (b) ferromagnetic wings under magnetic field H and the possibility of a quantum wing critical point (QWCP) or a marginal quantum critical point (MQCP), (c) a modulated magnetic phase AFM_Q and the possibility of a quantum tricritical point (QTCP). Panel (d) illustrates the case where the QTCP is avoided: the zero-temperature field-induced transition remains of the first order and a new phase emerges.

diagram of NbFe_2 by finely tuning the Nb-Fe ratio [37], and in the phase diagram of CeTiGe_3 by applying high pressure [17]. In both of these cases, however, further multiprobe investigation is limited by their experimentally restrictive tuning parameters, so the possibility remains that the QTCP is also avoided, that the zero-temperature field-induced transition remains of the first order, and that new phases appear as illustrated in Fig. 1(d).

In this Letter, we report on a new system that is easily tunable toward a QTCP. We study the Fe-substituted LaCrSb_3 system and demonstrate that a QTCP is approached, but ultimately avoided, and that a new magnetic phase appears above the putative QTCP. The use of chemical substitution instead of pressure allows for easier investigation of the magnetic order. Using neutron diffraction, we identify the new magnetic phase as a canted AFM order (cAFM). This is the first example of an avoided QTCP, providing further support for the idea that quantum criticality is ubiquitously avoided.

LaCrSb_3 is a ferromagnet ($T_C \sim 125$ K [43]; orthorhombic crystal structure, $Pbcm$ No. 57) with intricate magnetic properties. It does not obey the Curie-Weiss law above T_C and has a smaller saturation moment than free ionic Cr, suggesting some degree of itinerant magnetism [44–47]. Giant anomalous Hall conductivity was recently reported and arises from Cr-d dominated nearly dispersionless bands in the vicinity of the Fermi level [48,49]. Neutron diffraction revealed the spontaneous reorientation of moments from c to b at $T_{SR} = 95$ K. We will refer to the ground state phase as FM_b , although there is a small AFM component resulting in a tilt (18°) of the moments toward the c axis that subsists at least up to 7 T [50]. Its complicated magnetic structure involving both FM and AFM interactions makes LaCrSb_3 a natural candidate for achieving a QTCP. Pressure studies revealed a robust ferromagnetic ordering, requiring 26.5 GPa to be suppressed [51,52]. On the other hand, the magnetic order can be modified by various chemical substitutions [51,53–55]. Somewhat counterintuitively, given that Fe often enhances FM interactions, Fe substitution causes the most dramatic change in the magnetization and appears to strengthen AFM interactions in this system [53].

For this study we grew single crystals of $\text{LaCr}_{1-x}\text{Fe}_x\text{Sb}_3$ with nominal substitutions between 0 and 0.6 in steps of 0.05 following Ref. [51]. Energy-dispersive x-ray spectroscopy (EDX) was used to determine the Fe content that appeared to follow a linear function $x_{\text{EDX}} = 0.575x_{\text{nominal}}$ (see [56] Notes 1 and 2, Fig. S1). The x values discussed in this Letter are calculated from this linear relationship. We map the temperature-chemical substitution-magnetic field ($T-x-H$) phase diagram with bulk magnetization and resistivity measurements (experimental details given in [56]). Fe substitution suppresses T_C ; however, an FM-QCP is avoided by the appearance of a tricritical point (TCP) at which the transition becomes of the first order and

by the appearance of an AFM phase. The TCP can be driven to lower temperatures upon increasing Fe content and magnetic field. A QTCP, however, is avoided as the transition remains of the first order at low enough temperature. A new canted magnetic phase (cAFM) appears above the putative QTCP region. The phase diagram of $\text{LaCr}_{1-x}\text{Fe}_x\text{Sb}_3$ provides a road map for discovering magnetic canting in other materials due to the emergence of a cAFM phase near an avoided FM-AFM QTCP.

Phase diagram—Figure 2(a) shows the $T-x$ phase diagram of $\text{LaCr}_{1-x}\text{Fe}_x\text{Sb}_3$ determined from low-field (0.1 T) $M(T)$ measurements that are consistent with zero field $\rho(T)$ (see [56] Note 5, Fig. S6). When $x \leq 0.09$, the ground state is FM_b [Fig. 2(b)]. As substitution is increased, the FM transition becomes of the first order (see [56] Note 6). When $x \geq 0.12$, the $M(T)$ curve exhibits a precipitous downturn in M_b indicating the appearance of an AFM_b state where the b components of the moments are now antiferromagnetically aligned [Fig. 2(c)]. We determined the magnetic structure of the AFM_b phase with

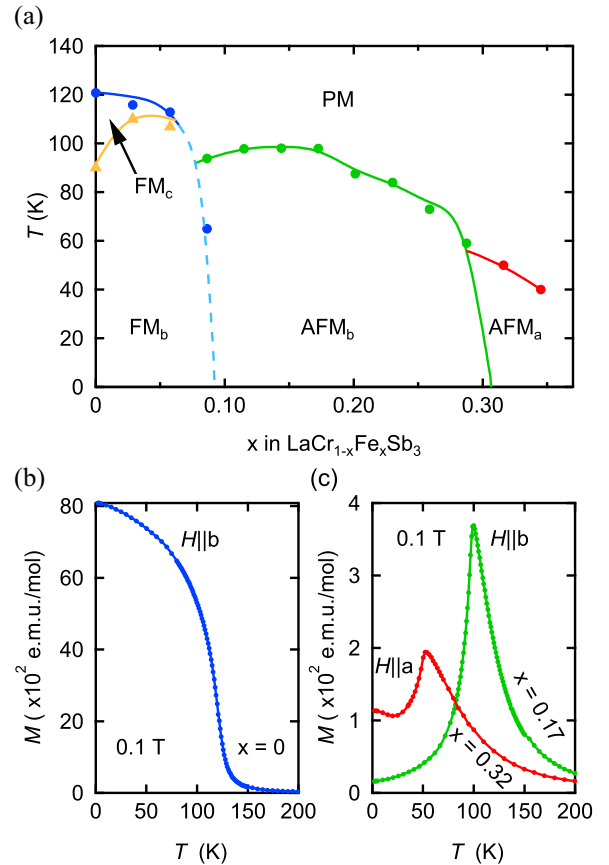


FIG. 2. (a) The temperature vs Fe-substitution phase diagram showing the ferromagnetic (FM_b and FM_c), and antiferromagnetic (AFM_b and AFM_a) regions. The lines are guides to the eye. The dashed line indicates a first order transition. (b)–(c) Representative magnetization as a function of temperature, $M(T)$, curves of the (b) FM_b , as well as the (c) AFM_b and AFM_a phases measured at 0.1 T.

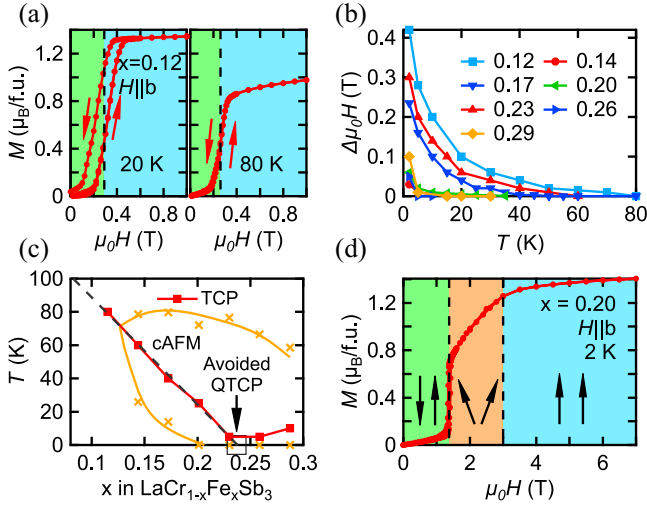


FIG. 3. (a) Magnetization as a function of applied magnetic field, $M(H)$, at 20 K and 80 K for $x = 0.12$. Red arrows indicate increasing and decreasing field directions. Green and blue regions indicate the antiferromagnetic (AFM_b) and ferromagnetic (FM_b) phases, respectively. (b) The hysteresis widths extracted from similar $M(H)$ measurements as a function of temperature for different x values. (c) Red squares indicate the x dependence of the temperature of the tricritical point (TCP). The position of the avoided QTCP is marked by the black open square. Orange crosses represent the maximum and minimum temperature between which the cAFM phase is observed. Each point is observed at a different field. (d) $M(H)$ at 2 K for $x = 0.20$. The green, orange, and blue regions denote the AFM_b , cAFM, and FM_b phases, respectively. Black arrows schematically represent the alignment of magnetic moments in each region.

single crystal neutron diffraction (see [56] Note 7). The easy moment direction changes to the a axis for $x > 0.29$ (AFM_a) [Fig. 2(c)].

The TCP at which the FM transition changes from second to first order exists at zero magnetic field, but is better revealed under field. Figure 3(a) shows $M(H)$ curves for $x = 0.12$. At low temperatures, the spin-flip transition between the AFM_b and polarized FM_b states exhibits hysteresis indicating the first order nature of the transition. This hysteresis is also observed in $\rho(H)$ (see [56] Fig. S7). Increasing the temperature causes the magnitude of the hysteresis to diminish. The hysteresis vanishes at 80 K, taken as the temperature of the TCP (T_{TCP}). The temperature dependence of the hysteresis for $0.12 \leq x \leq 0.29$ is shown in Fig. 3(b). With increasing x , the hysteresis is reduced and the temperature at which the hysteresis disappears shifts to lower temperature, indicating a decrease of T_{TCP} . Figure 3(c) shows T_{TCP} as a function of x and reveals an almost perfectly linear trend toward zero temperature where a QTCP is expected to occur. If a QTCP were to exist in the $\text{LaCr}_{1-x}\text{Fe}_x\text{Sb}_3$ system, substitutions beyond the x of the QTCP are expected to have a line of AFM-QCPs without hysteresis [Fig. 1(c)]. Instead, for $x > 0.23$, the hysteresis remains and T_{TCP} slowly increases,

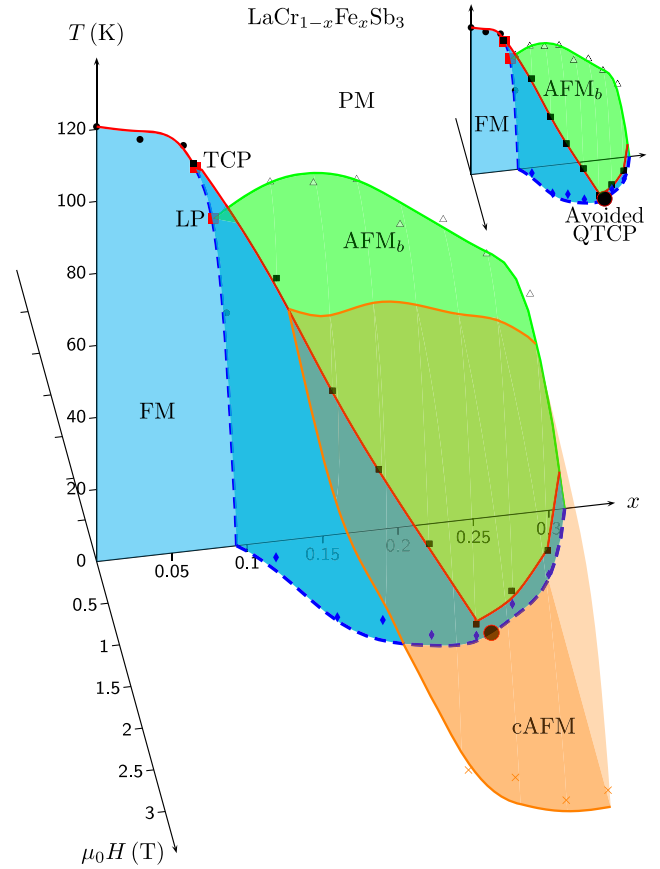


FIG. 4. The temperature-chemical substitution-magnetic field ($T - x - H$) phase diagram for the $\text{LaCr}_{1-x}\text{Fe}_x\text{Sb}_3$ system. The green and orange domes enclose the AFM_b and cAFM phases, respectively. The dashed blue line indicates a first order transition. The black squares denote tricritical points (TCPs) that are joined by the red tricritical line. The black dot is a placeholder for the putative position of the avoided QTCP. The diagram without the cAFM phase region is shown on the top right.

indicating the persistence of a first order transition and therefore the avoidance of a QTCP.

Figure 3(c) also depicts the canted AFM (cAFM) phase surrounding the tricritical line. The orange region in Fig. 3(d) defines the cAFM phase that is characterized by a region of linearly increasing $M(H)$ between the AFM_b and FM_b states. The cAFM state also appears as a broad bump in $\rho(H)$ (see [56] Fig. S7) as well as a kink in the $M(T)$ curve. The alignment of the magnetic moments in these different phases was determined by neutron diffraction (see [56] Note 7) and is shown schematically by the black arrows. While the hysteresis and T_{TCP} diminish with increasing x up to $x = 0.23$, the cAFM phase expands and appears to bury the putative QTCP.

The resulting three-dimensional $T - x - H$ phase diagram of $\text{LaCr}_{1-x}\text{Fe}_x\text{Sb}_3$ is shown in Fig. 4. The $T - H$ phase diagrams that were compiled to create this three-dimensional phase diagram are shown in [56] Fig. S15. From these phase diagrams, as well as the $M(H)$ curves, we

can see the growth of the cAFM dome as substitution is increased. Although a cAFM phase can be viewed as a combination of FM and AFM orders, it is interesting to note that the cAFM phase is not observed at low fields near the boundary between the FM and AFM regions. Instead, it only emerges near the tricritical line, when the TCP is driven toward lower temperatures. This suggests that the cAFM dome might originate from the putative QTCP, even though the latter is ultimately avoided. The experimental study of quantum fluctuations across the phase diagram will shed light on the question of the relationship between cAFM and QTCP.

Discussion—The magnetic phase diagram of $\text{LaCr}_{1-x}\text{Fe}_x\text{Sb}_3$ shows an FM-QCP avoided by a first order FM transition and the subsequent appearance of a modulated magnetic phase. Both features have been observed experimentally in other compounds [13,16] and studied theoretically [7,25,29,38]. The use of chemical substitution instead of pressure, and the fact that relatively large single crystals can be grown, make $\text{LaCr}_{1-x}\text{Fe}_x\text{Sb}_3$ an ideal platform for multiprobe investigations of quantum criticality.

$\text{LaCr}_{1-x}\text{Fe}_x\text{Sb}_3$ is the first example of an avoided QTCP. Previous experiments have suggested the existence of a QTCP in $\text{Nb}_{1-y}\text{Fe}_{2+y}$ [37] and CeTiGe_3 [17]. The complication of high pressure and limited range of substitution in these systems, however, restricted detailed studies in the proximity of the QTCP. As a consequence, it is possible that the QTCP is also avoided in these cases. The scenario in which achieving quantum criticality was initially reported, but later found to be avoided, has occurred for both AFM and FM-QCPs. For a long time, YbRh_2Si_2 was believed to be a clear example of an AFM-QCP [64,65], then a superconducting phase was discovered in place of the QCP upon reaching temperatures below $T = 2$ mK [66,67]. ZrZn_2 was once believed to be an example of an FM-QCP [68], until tricritical wings were observed upon reaching lower temperatures in higher quality samples [8,10,69,70]. If samples beyond $x = 0.23$ were not produced, or if the hysteresis in the AFM-FM transition did not appear above $T = 2$ K, or if magnetization and neutron measurements revealing the cAFM phase could not be performed easily, one would have concluded the existence of a QTCP in $\text{LaCr}_{1-x}\text{Fe}_x\text{Sb}_3$.

The mechanism behind the emergence of superconductivity near quantum critical points remains unknown. In the case of the appearance of AFM_Q phases instead of FM QCPs, the importance of quantum effects [24,26,27, 71–73], the influence of magnetic anisotropy [14,27], or specific band structure features have been proposed [28,74,75], but distinguishing between them is difficult [26]. The fact that some of these phases subsist up to relatively high temperatures is at odds with a purely quantum effect. In the case of the cAFM phase observed here, it is likely that multiple effects contribute simultaneously to the avoidance of quantum criticality. Further studies will tell whether a QTCP can be obtained under

special crystalline symmetries or disorder, as proposed for FM-QCP [30–32,35,36].

Finally, we note that our results provide a route to drive a system toward canted AFM phases. Magnetic canting has recently attracted attention as a way to tune the anomalous Hall effect (AHE) due to the scaling relation of the AHE with magnetization [76,77], or to induce a chiral Hall effect and corresponding chiral magneto-optical effects [78]. Noncollinear antiferromagnets can display an intrinsic AHE from nonzero Berry curvature [79]. When the canting is small, the sign of the Hall effect can be switched easily, which could enable new spintronic applications [80]. The canted magnetization also gives rise to novel magneto-thermoelectric effects [81]. The phase diagram of $\text{La}(\text{Cr}, \text{Fe})\text{Sb}_3$ where the emergence of a cAFM phase is observed in the vicinity of a FM-AFM QTCP provides a general guide to induce magnetic canting in other magnetic materials. In the past, the pursuit of AFM-QCP led to the discovery of unconventional superconductivity. Similarly, our results show that following the FM-AFM tricritical line can lead to the discovery of complex spin textures.

Acknowledgments—We thank M. Brando, D. Belitz, T. R. Kirkpatrick, A. G. Green, F. Krüger, and I. M. Vishik for useful discussion. R. R. U. and V. T. acknowledge support from the UC Laboratory Fees Research Program (LFR-20-653926) and the UC Davis Physics Liquid Helium Laboratory Fund. A portion of this research used resources at the High Flux Isotope Reactor, a DOE Office of Science User Facility operated by the Oak Ridge National Laboratory. Part of this study was carried out at the UC Davis Advanced Materials Characterization and Testing Laboratory (AMCaT), under the NSF Major Research Instrumentation grant, MRI-1725618. The authors thank Kashyap Ganesan for discussions and training on the EDS measurement.

-
- [1] P. Monthoux, D. Pines, and G. G. Lonzarich, Superconductivity without phonons, *Nature (London)* **450**, 1177 (2007).
 - [2] J. Paglione and R. L. Greene, High-temperature superconductivity in iron-based materials, *Nat. Phys.* **6**, 645 (2010).
 - [3] P. Gegenwart, Q. Si, and F. Steglich, Quantum criticality in heavy-fermion metals, *Nat. Phys.* **4**, 186 (2008).
 - [4] G. R. Stewart, Unconventional superconductivity, *Adv. Phys.* **66**, 75 (2017).
 - [5] S. S. Saxena, P. Agarwal, K. Ahilan, F. M. Grosche, R. K. W. Haselwimmer, M. J. Steiner, E. Pugh, I. R. Walker, S. R. Julian, P. Monthoux, G. G. Lonzarich, A. Huxley, I. Sheikin, D. Braithwaite, and J. Flouquet, Superconductivity on the border of itinerant-electron ferromagnetism in UGe_2 , *Nature (London)* **406**, 587 (2000).
 - [6] E. Slooten, T. Naka, A. Gasparini, Y. K. Huang, and A. de Visser, Enhancement of superconductivity near the ferromagnetic quantum critical point in UCoGe , *Phys. Rev. Lett.* **103**, 097003 (2009).

- [7] M. Brando, D. Belitz, F. M. Grosche, and T. R. Kirkpatrick, Metallic quantum ferromagnets, *Rev. Mod. Phys.* **88**, 025006 (2016).
- [8] M. Uhlarz, C. Pfleiderer, and S. M. Hayden, Quantum phase transitions in the itinerant ferromagnet ZrZn_2 , *Phys. Rev. Lett.* **93**, 256404 (2004).
- [9] V. Taufour, D. Aoki, G. Knebel, and J. Flouquet, Tricritical point and wing structure in the itinerant ferromagnet UGe_2 , *Phys. Rev. Lett.* **105**, 217201 (2010).
- [10] N. Kabeya, H. Maekawa, K. Deguchi, N. Kimura, H. Aoki, and N. K. Sato, Non-Fermi liquid state bounded by a possible electronic topological transition in ZrZn_2 , *J. Phys. Soc. Jpn.* **81**, 073706 (2012).
- [11] Y. Yamaji, T. Misawa, and M. Imada, Quantum and topological criticalities of Lifshitz transition in two-dimensional correlated electron systems, *J. Phys. Soc. Jpn.* **75**, 094719 (2006).
- [12] S. Lausberg, J. Spehling, A. Steppke, A. Jesche, H. Luetkens, A. Amato, C. Baines, C. Krellner, M. Brando, C. Geibel, H. H. Klauss, and F. Steglich, Avoided ferromagnetic quantum critical point: Unusual short-range ordered state in CeFePO , *Phys. Rev. Lett.* **109**, 216402 (2012).
- [13] H. Kotegawa, T. Toyama, S. Kitagawa, H. Tou, R. Yamauchi, E. Matsuoka, and H. Sugawara, Pressure-temperature-magnetic field phase diagram of ferromagnetic Kondo lattice CeRuPO , *J. Phys. Soc. Jpn.* **82**, 123711 (2013).
- [14] C. D. O'Neill, G. Abdul-Jabbar, D. Wermeille, P. Bourges, F. Krüger, and A. D. Huxley, Field-induced modulated state in the ferromagnet PrPtAl , *Phys. Rev. Lett.* **126**, 197203 (2021).
- [15] J.-G. Cheng, K. Matsubayashi, W. Wu, J. P. Sun, F. K. Lin, J. L. Luo, and Y. Uwatoko, Pressure induced superconductivity on the border of magnetic order in MnP , *Phys. Rev. Lett.* **114**, 117001 (2015).
- [16] V. Taufour, U. S. Kaluarachchi, R. Khasanov, M. C. Nguyen, Z. Guguchia, P. K. Biswas, P. Bonfã, R. De Renzi, X. Lin, S. K. Kim, E. D. Mun, H. Kim, Y. Furukawa, C.-Z. Wang, K.-M. Ho, S. L. Bud'ko, and P. C. Canfield, Ferromagnetic quantum critical point avoided by the appearance of another magnetic phase in LaCrGe_3 under pressure, *Phys. Rev. Lett.* **117**, 037207 (2016).
- [17] U. S. Kaluarachchi, V. Taufour, S. L. Bud'ko, and P. C. Canfield, Quantum tricritical point in the temperature-pressure-magnetic field phase diagram of CeTiGe_3 , *Phys. Rev. B* **97**, 045139 (2018).
- [18] H. Kotegawa, T. Uga, H. Tou, E. Matsuoka, and H. Sugawara, Avoided ferromagnetic quantum critical point in CeZn , *Phys. Rev. B* **106**, L180405 (2022).
- [19] A. Jesche, T. Ballé, K. Kliemt, C. Geibel, M. Brando, and C. Krellner, Avoided ferromagnetic quantum critical point: Antiferromagnetic ground state in substituted CeFePO , *Phys. Status Solidi (b)* **254**, 1600169 (2017).
- [20] E. Lengyel, M. E. Macovei, A. Jesche, C. Krellner, C. Geibel, and M. Nicklas, Avoided ferromagnetic quantum critical point in CeRuPO , *Phys. Rev. B* **91**, 035130 (2015).
- [21] M. Matsuda, F. Ye, S. E. Dissanayake, J.-G. Cheng, S. Chi, J. Ma, H. D. Zhou, J.-Q. Yan, S. Kasamatsu, O. Sugino, T. Kato, K. Matsubayashi, T. Okada, and Y. Uwatoko, Pressure dependence of the magnetic ground states in MnP , *Phys. Rev. B* **93**, 100405(R) (2016).
- [22] L. Xiang, E. Gati, S. L. Bud'ko, S. M. Saunders, and P. C. Canfield, Avoided ferromagnetic quantum critical point in pressurized $\text{La}_3\text{Ce}_2\text{Ge}_3$, *Phys. Rev. B* **103**, 054419 (2021).
- [23] H. Wang, T. B. Park, S. Shin, J. Kim, H. Lee, and T. Park, Temperature-pressure phase diagram of the ferromagnetic Kondo lattice compound $\text{CePtAl}_4\text{Si}_2$, *Phys. Rev. Mater.* **7**, 075003 (2023).
- [24] A. V. Chubukov, C. Pepin, and J. Rech, Instability of the quantum-critical point of itinerant ferromagnets, *Phys. Rev. Lett.* **92**, 147003 (2004).
- [25] D. Belitz, T. R. Kirkpatrick, and J. Rollbühler, Tricritical behavior in itinerant quantum ferromagnets, *Phys. Rev. Lett.* **94**, 247205 (2005).
- [26] G. J. Conduit, A. G. Green, and B. D. Simons, Inhomogeneous phase formation on the border of itinerant ferromagnetism, *Phys. Rev. Lett.* **103**, 207201 (2009).
- [27] U. Karahasanovic, F. Krüger, and A. G. Green, Quantum order-by-disorder driven phase reconstruction in the vicinity of ferromagnetic quantum critical points, *Phys. Rev. B* **85**, 165111 (2012).
- [28] M. M. Wysokinski, Mechanism for transitions between ferromagnetic and antiferromagnetic orders in d-electron metallic magnets, *Sci. Rep.* **9**, 19461 (2019).
- [29] D. Miserev, D. Loss, and J. Klinovaja, Instability of the ferromagnetic quantum critical point and symmetry of the ferromagnetic ground state in two-dimensional and three-dimensional electron gases with arbitrary spin-orbit splitting, *Phys. Rev. B* **106**, 134417 (2022).
- [30] T. R. Kirkpatrick and D. Belitz, Ferromagnetic quantum critical point in noncentrosymmetric systems, *Phys. Rev. Lett.* **124**, 147201 (2020).
- [31] H. Kotegawa, E. Matsuoka, T. Uga, M. Takemura, M. Manago, N. Chikuchi, H. Sugawara, H. Tou, and H. Harima, Indication of ferromagnetic quantum critical point in Kondo lattice CeRh_6Ge_4 , *J. Phys. Soc. Jpn.* **88**, 093702 (2019).
- [32] B. Shen, Y. Zhang, Y. Komijani, M. Nicklas, R. Borth, A. Wang, Y. Chen, Z. Nie, R. Li, X. Lu, H. Lee, M. Smidman, F. Steglich, P. Coleman, and H. Yuan, Strange-metal behaviour in a pure ferromagnetic Kondo lattice, *Nature (London)* **579**, 51 (2020).
- [33] C. Krellner, S. Lausberg, A. Steppke, M. Brando, L. Pedrero, H. Pfau, S. Tencé, H. Rosner, F. Steglich, and C. Geibel, Ferromagnetic quantum criticality in the quasi-one-dimensional heavy fermion metal YbNi_4P_2 , *New J. Phys.* **13**, 103014 (2011).
- [34] A. Steppke, R. Kuechler, S. Lausberg, E. Lengyel, L. Steinke, R. Borth, T. Luehmann, C. Krellner, M. Nicklas, C. Geibel, F. Steglich, and M. Brando, Ferromagnetic quantum critical point in the heavy-fermion metal $\text{YbNi}_4(\text{P}_{1-x}\text{As}_x)_2$, *Science* **339**, 933 (2013).
- [35] Y. Sang, D. Belitz, and T. R. Kirkpatrick, Disorder dependence of the ferromagnetic quantum phase transition, *Phys. Rev. Lett.* **113**, 207201 (2014).
- [36] T. Goko, C. J. Arguello, A. Hamann, T. Wolf, M. Lee, D. Reznik, A. Maisuradze, R. Khasanov, E. Morenzoni, and Y. J. Uemura, Restoration of quantum critical behavior by disorder in pressure-tuned $(\text{Mn,Fe})\text{Si}$, *npj Quantum Mater.* **2**, 44 (2017).

- [37] S. Friedemann, W. J. Duncan, M. Hirschberger, T. W. Bauer, R. Kuchler, A. Neubauer, M. Brando, C. Pfleiderer, and F. M. Grosche, Quantum tricritical points in NbFe₂, *Nat. Phys.* **14**, 62 (2017).
- [38] D. Belitz and T. R. Kirkpatrick, Quantum triple point and quantum critical end points in metallic magnets, *Phys. Rev. Lett.* **119**, 267202 (2017).
- [39] T. Misawa, Y. Yamaji, and M. Imada, YbRh₂Si₂: Quantum tricritical behavior in itinerant electron systems, *J. Phys. Soc. Jpn.* **77**, 093712 (2008).
- [40] T. Misawa, Y. Yamaji, and M. Imada, Spin fluctuation theory for quantum tricritical point arising in proximity to first-order phase transitions: Applications to heavy-fermion systems, YbRh₂Si₂, CeRu₂Si₂, and β -YbAlB₄, *J. Phys. Soc. Jpn.* **78**, 084707 (2009).
- [41] S. Hamann, J. Zhang, D. Jang, A. Hannaske, L. Steinke, S. Lausberg, L. Pedrero, C. Klingner, M. Baenitz, F. Steglich, C. Krellner, C. Geibel, and M. Brando, Evolution from ferromagnetism to antiferromagnetism in Yb(Rh_{1-x}Co_x)₂Si₂, *Phys. Rev. Lett.* **122**, 077202 (2019).
- [42] T. Moriya and K. Usami, Coexistence of ferro- and antiferromagnetism and phase-transitions in itinerant electron-systems, *Solid State Commun.* **23**, 935 (1977).
- [43] K. Hartjes, W. Jeitschko, and M. Brylak, Magnetic properties of the rare-earth transition metal antimonides LnVSb₃ and LnCrSb₃ (Ln = La-Nd, Sm), *J. Magn. Magn. Mater.* **173**, 109 (1997).
- [44] N. P. Raju, J. E. Greedan, M. J. Ferguson, and A. Mar, LaCrSb₃: A new itinerant electron ferromagnet with a layered structure, *Chem. Mater.* **10**, 3630 (1998).
- [45] M. Leonard, I. Dubenko, and N. Ali, Investigation of the ferromagnetism in RCrSb₃ (R = La, Ce, Pr, Nd), *J. Alloys Compd.* **303–304**, 265 (2000).
- [46] M. Richter, J. Ruzs, H. Rosner, K. Koepernik, I. Opahle, U. Nitzsche, and H. Eschrig, Unconventional metallic magnetism in LaCrSb₃, *J. Magn. Magn. Mater.* **272–276**, E251 (2004).
- [47] D. D. Jackson, M. Torelli, and Z. Fisk, Anisotropy in magnetic and transport properties of LaTSb₃ (T = Cr, V), *Phys. Rev. B* **65**, 014421 (2001).
- [48] N. Kumar, N. Lamba, J. Gayles, C. Le, P. Vir, S. N. Guin, Y. Sun, C. Felser, and C. Shekhar, Giant anomalous Hall conductivity in the itinerant ferromagnet LaCrSb₃ and the effect of f-electrons, *Adv. Quantum Technol.* **4**, 2100023 (2021).
- [49] W. Jiang, D. J. P. de Sousa, J.-P. Wang, and T. Low, Giant anomalous Hall effect due to double-degenerate quasiflat bands, *Phys. Rev. Lett.* **126**, 106601 (2021).
- [50] E. Granado, H. Martinho, M. S. Sercheli, P. G. Pagliuso, D. D. Jackson, M. Torelli, J. W. Lynn, C. Rettori, Z. Fisk, and S. B. Oseroff, Unconventional metallic magnetism in LaCrSb₃, *Phys. Rev. Lett.* **89**, 107204 (2002).
- [51] X. Lin, V. Taufour, S. L. Bud'ko, and P. C. Canfield, Suppression of ferromagnetism in the La(V_xCr_{1-x})Sb₃ system, *Philos. Mag.* **94**, 1277 (2014).
- [52] Z. E. Brubaker, J. S. Harvey, J. R. Badger, R. R. Ullah, D. J. Campbell, Y. Xiao, P. Chow, C. Kenney-Benson, J. S. Smith, C. Reynolds, J. Paglione, R. J. Zieve, J. R. Jeffries, and V. Taufour, Pressure-induced suppression of ferromagnetism in the itinerant ferromagnet LaCrSb₃, *Phys. Rev. B* **101**, 214408 (2020).
- [53] I. S. Dubenko, P. Hill, and N. Ali, Magnetic properties of LaCr_{1-x}M_xSb₃ (M = V, Mn, Fe, Cu, and Al), *J. Appl. Phys.* **89**, 7326 (2001).
- [54] D. D. Jackson and Z. Fisk, Effect of rare-earth doping in RCrSb₃ (R = La, Pr, Sm, and Gd), *Phys. Rev. B* **73**, 024421 (2006).
- [55] H. Chen, A. Narayan, L. Fang, N. P. Calta, F. Shi, D. Y. Chung, L. K. Wagner, W.-K. Kwok, and M. G. Kanatzidis, From complex magnetism ordering to simple ferromagnetism in two-dimensional LaCrSb₃ by hole doping, *Phys. Rev. B* **94**, 134411 (2016).
- [56] See Supplemental Material at <http://link.aps.org/supplemental/10.1103/PhysRevLett.133.096701>, which includes Refs. [57–63], for additional details regarding sample preparation, Fe substitution, powder x-ray diffraction, electrical resistivity, magnetization, and neutron diffraction measurements and additional phase diagrams.
- [57] P. C. Canfield, T. Kong, U. S. Kaluarachchi, and N. H. Jo, Use of frit-disc crucibles for routine and exploratory solution growth of single crystalline samples, *Philos. Mag.* **96**, 84 (2016).
- [58] M. J. Ferguson, R. W. Hushagen, and A. Mar, Crystal structures of La₃ZrSb₅, La₃HfSb₅, and LaCrSb₃. Structural relationships in ternary rare-earth antimonides, *J. Alloys Compd.* **249**, 191 (1997).
- [59] A. Jesche, M. Fix, A. Kreyssig, W. R. Meier, and P. C. Canfield, X-ray diffraction on large single crystals using a powder diffractometer, *Philos. Mag.* **96**, 2115 (2016).
- [60] B. H. Toby and R. B. Von Dreele, GSAS-II: The genesis of a modern open-source all purpose crystallography software package, *J. Appl. Crystallogr.* **46**, 544 (2013).
- [61] B. C. Chakoumakos, H. Cao, F. Ye, A. D. Stoica, M. Popovici, M. Sundaram, W. Zhou, J. S. Hicks, G. W. Lynn, and R. A. Riedel, Four-circle single-crystal neutron diffractometer at the high flux isotope reactor, *J. Appl. Crystallogr.* **44**, 655 (2011).
- [62] J. Perez-Mato, S. Gallego, E. Tasci, L. Elcoro, G. de la Flor, and M. Aroyo, Symmetry-based computational tools for magnetic crystallography, *Annu. Rev. Mater. Res.* **45**, 217 (2015).
- [63] J. Rodríguez-Carvajal, Recent advances in magnetic structure determination by neutron powder diffraction, *Physica (Amsterdam)* **192B**, 55 (1993).
- [64] J. Custers, P. Gegenwart, H. Wilhelm, K. Neumaier, Y. Tokiwa, O. Trovarelli, C. Geibel, F. Steglich, C. Pepin, and P. Coleman, The break-up of heavy electrons at a quantum critical point, *Nature (London)* **424**, 524 (2003).
- [65] P. Gegenwart, J. Custers, C. Geibel, K. Neumaier, T. Tayama, K. Tenya, O. Trovarelli, and F. Steglich, Magnetic-field induced quantum critical point in YbRh₂Si₂, *Phys. Rev. Lett.* **89**, 056402 (2002).
- [66] E. Schuberth, M. Tippmann, L. Steinke, S. Lausberg, A. Steppke, M. Brando, C. Krellner, C. Geibel, R. Yu, Q. Si, and F. Steglich, Emergence of superconductivity in the canonical heavy-electron metal YbRh₂Si₂, *Science* **351**, 485 (2016).
- [67] D. H. Nguyen, A. Sidorenko, M. Taupin, G. Knebel, G. Lapertot, E. Schuberth, and S. Paschen, Superconductivity in an extreme strange metal, *Nat. Commun.* **12**, 4341 (2021).

- [68] T. F. Smith, J. A. Mydosh, and W. E. P., Destruction of ferromagnetism in ZrZn_2 at high pressure, *Phys. Rev. Lett.* **27**, 1732 (1971).
- [69] S. Takashima, M. Nohara, H. Ueda, N. Takeshita, C. Terakura, F. Sakai, and H. Takagi, Robustness of non-Fermi-liquid behavior near the ferromagnetic critical point in clean ZrZn_2 , *J. Phys. Soc. Jpn.* **76**, 043704 (2007).
- [70] N. Kabeya, H. Maekawa, K. Deguchi, N. Kimura, H. Aoki, and N. K. Sato, Phase diagram of the itinerant-electron ferromagnet ZrZn_2 , *Phys. Status Solidi B* **250**, 654 (2013).
- [71] D. Belitz, T. R. Kirkpatrick, and T. Vojta, First order transitions and multicritical points in weak itinerant ferromagnets, *Phys. Rev. Lett.* **82**, 4707 (1999).
- [72] D. Belitz, T. R. Kirkpatrick, and J. Rollbühler, Tricritical behavior in itinerant quantum ferromagnets, *Phys. Rev. Lett.* **94**, 247205 (2005).
- [73] S. J. Thomson, F. Krüger, and A. G. Green, Helical glasses near ferromagnetic quantum criticality, *Phys. Rev. B* **87**, 224203 (2013).
- [74] K. G. Sandeman, G. G. Lonzarich, and A. J. Schofield, Ferromagnetic superconductivity driven by changing Fermi surface topology, *Phys. Rev. Lett.* **90**, 167005 (2003).
- [75] F. Honda, N. Metoki, T. D. Matsuda, Y. Haga, and Y. Onuki, Long-period, longitudinal spin density modulation in an itinerant 5f magnetic compound UCu_2Si_2 , *J. Phys. Condes. Matter* **18**, 479 (2006).
- [76] S.-K. Bac, K. Koller, F. Lux, J. Wang, L. Riney, K. Borisiak, W. Powers, M. Zhukovskiy, T. Orlova, M. Dobrowolska, J. K. Furdyna, N. R. Dilley, L. P. Rokhinson, Y. Mokrousov, R. J. McQueeney, O. Heinonen, X. Liu, and B. A. Assaf, Topological response of the anomalous Hall effect in MnBi_2Te_4 due to magnetic canting, *npj Quantum Mater.* **7**, 46 (2022).
- [77] N. Nagaosa, J. Sinova, S. Onoda, A. H. MacDonald, and N. P. Ong, Anomalous Hall effect, *Rev. Mod. Phys.* **82**, 1539 (2010).
- [78] J. Kipp, K. Samanta, F. R. Lux, M. Merte, D. Go, J.-P. Hanke, M. Redies, F. Freimuth, S. Blugel, M. Lezaic, and Y. Mokrousov, The chiral Hall effect in canted ferromagnets and antiferromagnets, *Commun. Phys.* **4**, 99 (2021).
- [79] H. Chen, Q. Niu, and A. H. MacDonald, Anomalous Hall effect arising from noncollinear antiferromagnetism, *Phys. Rev. Lett.* **112**, 017205 (2014).
- [80] S. Nakatsuji, N. Kiyohara, and T. Higo, Large anomalous Hall effect in a non-collinear antiferromagnet at room temperature, *Nature (London)* **527**, 212 (2015).
- [81] W. Lin, J. He, B. Ma, M. Matzelle, J. Xu, J. Freeland, Y. Choi, D. Haskel, B. Barbiellini, A. Bansil, G. A. Fiete, J. Zhou, and C. L. Chien, Evidence for spin swapping in an antiferromagnet, *Nat. Phys.* **18**, 800 (2022).